Halogen Interactions

DOI: 10.1002/anie.200805739

The Nature of Halogen···Halogen Interactions: A Model Derived from Experimental Charge-Density Analysis**

*Thai Thanh Thu Bui, Slimane Dahaoui, Claude Lecomte, Gautam R. Desiraju, and Enrique Espinosa**

In memory of Niels K. Hansen (1950–2007)

That non-directional pair-wise atom–atom potentials containing only attractive (r^{-6} dispersion term) and repulsive (inverse-power or exponential term) contributions are insufficient to model Cl···Cl interactions in molecular crystals was appreciated 40 years ago.[1] The layered orthorhombic crystal structures (space group *Cmca*) of the halogens (Cl_2, Br_2, I_2) cannot be anticipated with isotropic potentials (which would predict, for example, cubic packings, such as the $Pa\bar{3}$ structure as seen for N_2, NO, and CO),[2] and consideration of previously postulated quadrupole–quadrupole interactions[3] did not resolve this issue. Two possibilities have commonly been invoked to explain these anomalous halogen-atom contacts. Williams and Hsu proposed that halogen atoms in molecular crystals are weakly bonded (for Cl···Cl interactions, this bonding component was estimated to be around 3% of the energy of a Cl–Cl covalent bond).[4] Such bonding was then considered to be the origin of the crystal anisotropy. Nyburg and Wong-Ng, on the other hand, proposed a model that assigned anisotropic non-bonded radii (Scheme 1a) to Cl atoms in crystals.[5] The elliptically shaped atoms were then related to the origin of the anisotropy in the crystal packing. Over the years, all interpretations of Cl···Cl interactions in crystals invoked one or the other of these two models.[6] However, it is difficult to distinguish computationally between them: the Williams model proposes an increased attraction while the Nyburg model proposes a decreased repulsion between non-bonded atoms. Is there any real difference between these situations in an empirical or semi-empirical computational approach? An experimental analysis is required to differentiate these possibilities, as we pointed recently for Cl···Cl interactions.[7]

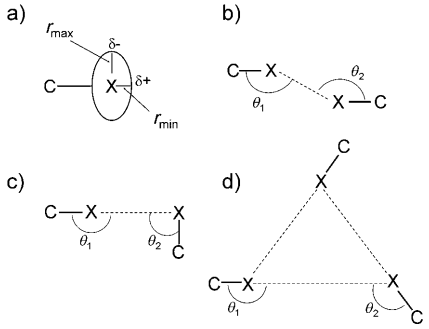

Scheme 1. Halogen···halogen interactions. a) Polar flattening effect, showing different atomic radii (r) associated with oppositely polarized regions along perpendicular directions, b) type-I interactions ($\theta_1 \approx \theta_2$), c) type-II interactions ($\theta_1 \approx 180°$, $\theta_2 \approx 90°$), d) X_3 synthon ($\theta_1 \approx 180°$, $\theta_2 \approx 120°$).

The geometrical characteristics of halogen-atom interactions (C–X···X–C, X = Cl, Br, I) have been identified as belonging to two different types (type-I and type-II; Scheme 1) based on the geometrical C–X···X angles θ_1 and θ_2.[8] Type-I interactions (Scheme 1b) are symmetrical and occur almost always around a crystallographic inversion centre. These interactions are of the van der Waals type, such that the shortest among these (for Cl···Cl, shorter than 3.30 Å) are actually repulsive. Type-II interactions (Scheme 1c), which are commonly associated with crystallographic screw axes and glide planes, may be understood according to a model that assigns a positive polarization in the polar region of the Cl atom and a negative polarization in its equatorial region (Scheme 1a). Type-II contacts are then understood as an attractive $Cl^{\delta+}\cdots Cl^{\delta-}$ interaction and correspond to the Williams model. There is circumstantial evidence that such a depiction is applicable for type-II Cl···Cl interactions. For example, the likelihood of a type-II interaction increases over type-I, on proceeding from Cl to I, in other words as the halogen atom becomes more polarizable.[9] Also, in unsymmetrical halogen···halogen type-II contacts (I···Br, Cl···Br, I···Cl), the θ_2 angle (smaller angle) occurs more often at the lighter halogen atom, and this is the preferred possibility in that the heavier halogen is polarized positively and the lighter halogen negatively.[9] Further, there is ample evidence of supramolecular synthons of the Cl_3, Br_3, and I_3 type (Scheme 1d) in crystal engineering.[10]

[*] T. T. T. Bui, Dr. S. Dahaoui, Prof. C. Lecomte, Prof. E. Espinosa
Laboratoire de Cristallographie, Résonance Magnétique et Modélisations (UMR 7036), Nancy Université
Faculté des Sciences et Techniques, BP 239, Boulevard des Aiguillettes
54506 Vandoeuvre-lès-Nancy (France)
Fax: (+33) 383-406492
E-mail: enrique.espinosa@crm2.uhp-nancy.fr
Prof. G. R. Desiraju
School of Chemistry, University of Hyderabad
Hyderabad 500 046 (India)

[**] This work has been supported by the French Agence Nationale de la Recherche (grant ANR-08-BLAN-0091-01). G.R.D. thanks the DST, New Delhi, for the award of a J. C. Bose Fellowship. T.T.T.B. thanks the French Ministry of Research for a doctoral fellowship.

Supporting information for this article is available on the WWW under http://dx.doi.org/10.1002/anie.200805739.

Within this framework, both the Williams and the Nyburg models are based on the anisotropy of the electron density around halogen nuclei and this in turn leads to the polar flattening effect. As depicted in Scheme 1a, this effect is understood either as arising from different polarizations (Williams model) or from anisotropic van der Waals radii (Nyburg model). Accordingly, the distinctive feature between these two models is the interpretation of the effect (attractive or repulsive) induced by this anisotropy. In this context, the crystal structure of hexachlorobenzene, C_6Cl_6, and the isostructural C_6Br_6 and C_6I_6 are interesting. The X···X contacts in these crystal structures cannot be classified strictly as being either pure type-I or type-II using geometrical criteria. As a major feature, triangular X_3 synthons appear as important intermolecular building units. The C_6X_6 crystal packing is governed by π···π and X···X interactions, the X···X appearing weaker than the π···π interactions, as shown by the bending of the C_6Cl_6 crystals upon stress application.[11] However, despite their weakness, the directionality of the X···X interactions seems to play a crucial role in achieving a columnar assembly of stacked C_6X_6 molecules.

In our inquiry for a better insight into the nature of Cl···Cl interactions, we undertook the accurate high-resolution X-ray diffraction analysis of C_6Cl_6. This compound was selected to study the fundamental characteristics of halogen···halogen interactions,[12] namely directionality and strength. In such a study extremely high-quality experimental data are required because the interaction of interest is very weak. Atomic multipolar expansions[13] were used to reconstruct the crystalline charge density $\rho(\mathbf{r})$. For Cl atoms, two quadrupoles and two octupoles are the most relevant terms to recover the observed anisotropic $\rho(\mathbf{r})$ features in the C_6Cl_6 crystal structure. From the multipolar model, Figure 1 shows the total electron density, $\rho(\mathbf{r})$, and the static deformation electron density with respect to the spherical distribution of the isolated configuration, $\Delta\rho(\mathbf{r}) = \rho(\mathbf{r}) - \rho_{\text{spherical}}(\mathbf{r})$, for the three independent Cl atoms.

While the $\rho(\mathbf{r})$ maps in Figure 1 confirm the polar flattening effect (Scheme 1a), the corresponding $\Delta\rho(\mathbf{r})$ maps show the δ^+ and δ^- regions, as observed in chloranil.[14] All these systematic manifestations indeed have a common origin—the anisotropic electron distribution that is inherent in the bonded halogen atom. The three $\Delta\rho(\mathbf{r})$ deformations shown in Figure 1 are qualitatively similar (in the red regions $\rho(\mathbf{r})$ is in deficiency with respect to an isolated atom, and in the blue ones it is in excess). Beyond the extension of the red zones, the main difference between the $\Delta\rho(\mathbf{r})$ deformations is the dimension and the relative position of the excess electron density within the torus-like shape around the bonding axis.

In the region of the X_3 synthon, the $\Delta\rho(\mathbf{r})$ map clearly shows the orientations of the δ^- and δ^+ regions of the Cl atoms (Figure 2a). Electron excess and electron deficient regions face each other along the three synthon edges, suggesting directional $\delta^+\cdots\delta^-$ interactions and classifying the X_3 synthon as a co-operative manifestation of three side-on type-II interactions. In the regions of the intermolecular Cl1···Cl1, Cl2···Cl2, and Cl3···Cl3 contacts (Figure 2a), the relative orientation of the polarized δ^+ and δ^- zones is different, showing a side–side geometry that is accordingly classified as type-I (Table 1).

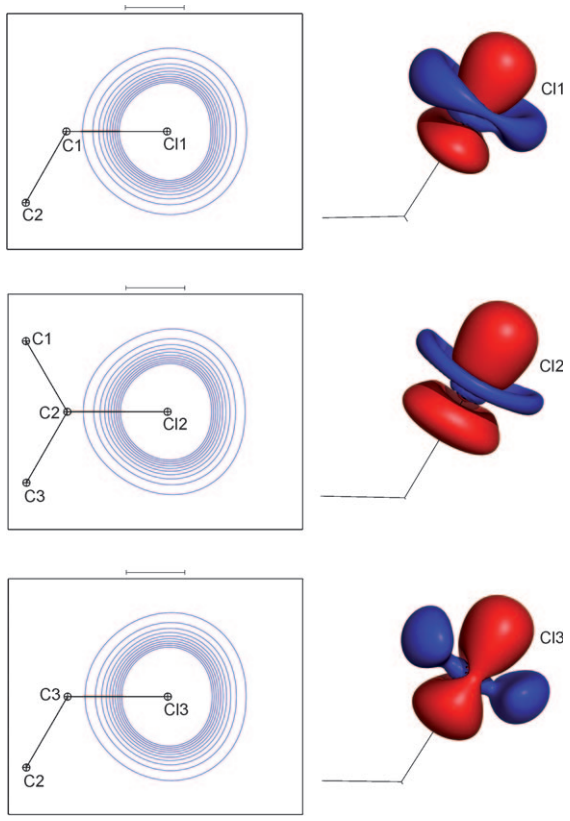

Figure 1. Maps of $\rho(\mathbf{r})$ (left) and $\Delta\rho(\mathbf{r})$ (right) for Cl atoms in the C_6Cl_6 crystal structure. In the $\rho(\mathbf{r})$ maps (contours each 0.1 e Å^{-3}), the r_{max} and r_{min} radii (in Å) and the r_{min}/r_{max} ratio at the first contour are, respectively: Cl1 (1.42, 1.36, 0.958), Cl2 (1.45, 1.32, 0.910), and Cl3 (1.43, 1.34, 0.937). The spherical model has a value of $r_{sph} = 1.42$ Å at the same contour. The $\Delta\rho(\mathbf{r})$ iso-surfaces are drawn at ± 0.05 e Å^{-3}. Blue and red indicate positive (electron excess, δ^-) and negative (electron deficiency, δ^+) regions, respectively.

Within the framework of quantum theory, the topological analysis of the electron density distribution[15] defines a unique and complete partition of the molecular space in basins Ω that, being separated by zero-flux surfaces S of $\rho(\mathbf{r})$,[16] behave as proper open quantum systems and define atoms in molecules.[17,15] According to this description, an immediate consequence of a bonding interaction is the existence of a bond path between the atoms and the concomitant bond critical point (BCP) along this direction, where $\rho(\mathbf{r})$ exhibits a saddle topology. The observation of BCPs is thus distinctive of interatomic bonding interactions[18] and the topological properties of $\rho(\mathbf{r})$ at BCP permit a characterization of the interaction.[15] Six independent BCPs associated with Cl···Cl bonding interactions are observed. The magnitudes of both the electron density ρ_{BCP} and the Laplacian $\nabla^2\rho_{BCP}$ are small ($0.03 < \rho_{BCP} < 0.06$ e Å^{-3} and $0.3 < \nabla^2\rho_{BCP} < 0.6$ e Å^{-5}), falling within the range of very weak hydrogen bonds.[19–21] In addition to the data quality, the confidence in these small topological characteristics also relies on the systematic trends appearing for all six independent Cl···Cl interactions even though they are at the limit

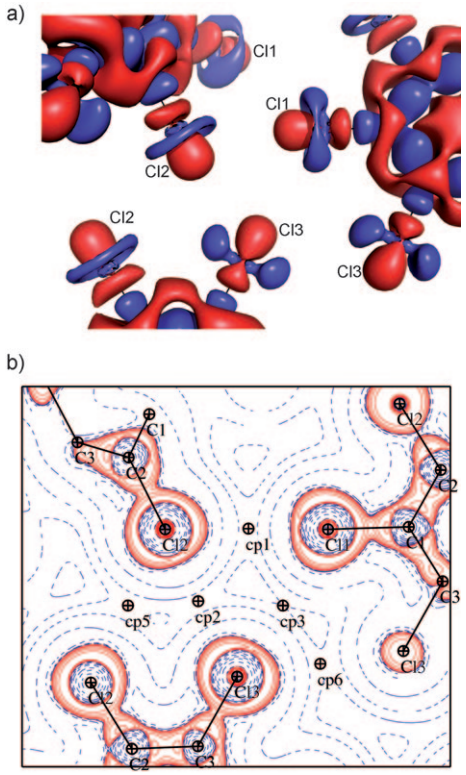

Figure 2. Experimental a) $\Delta\rho(\mathbf{r})$ and b) $\nabla^2\rho(\mathbf{r})$ maps in the X_3 synthon plane. The three other symmetry related Cl atoms depicted lie 0.33 (Cl2), 0.74 (Cl3), and 2.11 (Cl1) Å out of the synthon plane. Positive and negative values are represented in blue and red colors. $\Delta\rho(\mathbf{r})$ isosurfaces are drawn at ± 0.05 e Å^{-3} and $\nabla^2\rho(\mathbf{r})$ contours (e Å^{-5}) in logarithmic scale. Along with the synthon, side–side Cl···Cl interactions also appear in (a) and (b); Cl1···Cl1 does not appear in (b) because of the large out-of-plane distance of the second Cl1 atom. In (b), only Cl···Cl BCPs (⊕ symbols) are depicted (cp5 and cp6 are projected on the plane, and cp4 is not represented). cp = critical point.

of the experimental accuracy[22] that can be reached nowadays in experimental charge density analysis.

The $\nabla^2\rho(\mathbf{r})$ map plotted on the X_3 synthon plane (Figure 2b) indicates the regions where $\rho(\mathbf{r})$ is locally concentrated ($\nabla^2\rho(\mathbf{r}) < 0$) or depleted ($\nabla^2\rho(\mathbf{r}) > 0$). While Cl···Cl interactions in intermolecular regions show $\nabla^2\rho(\mathbf{r}) > 0$ (as other types of closed-shell interactions do),[15] $\nabla^2\rho(\mathbf{r}) < 0$ is observed for shared-shell interactions (C–Cl covalent bonds). Positive and negative regions are also observed around the nuclei, displaying alternating shells of charge concentration and depletion.[15] The valence-shell charge concentration (VSCC) of each Cl atom is thus represented by an outer anisotropic region where $\nabla^2\rho(\mathbf{r}) < 0$. The analysis of the $-\nabla^2\rho(\mathbf{r})$ function applied to the VSCC of an atom permits an identification of its local charge concentration (CC) and charge depletion (CD) zones.[23,15] Whereas CC regions appear on both sides of each Cl atom, perpendicular to the covalent bond axis, CD regions are observed along the bond axis, behind the nucleus, just in front of the intermolecular $\nabla^2\rho(\mathbf{r}) > 0$ region (Figure 2b), as observed in solid Cl_2.[24] Accordingly, the topology of $-\nabla^2\rho(\mathbf{r})$, with the CC and CD regions facing each other along the three directions of the synthon, permits the geometry of the X_3 synthon to be predicted. This picture nicely matches the $\Delta\rho$ map (Figure 2a) and the polar flattening effect (Scheme 1a). The CC magnitude and the CD depth are related in a straightforward way to the nucleophile–electrophile interaction.[25,15] Along the Cl···Cl bond paths, the local maxima of $-\nabla^2\rho(\mathbf{r})$ at both sides of each chlorine nucleus (CC regions) and the values of the function at the saddle point, placed along its bonding axis direction behind the nucleus (CD region), are (in e Å^{-5}): Cl1 (16.3, 17.5, and 5.5), Cl2 (15.8, 15.2, and 7.3) and Cl3 (16.0, 16.2, and 8.2). In the Cl_3 synthon, the differences $\Delta(-\nabla^2\rho) = (-\nabla^2\rho)_{max} - (-\nabla^2\rho)_{saddle}$ corresponding to the CC and CD regions facing to each other (Figure 2) follow the series Cl1···Cl2, Cl2···Cl3, and Cl3···Cl1 ($\Delta(-\nabla^2\rho) = 10.2$, 8.8, and 8.1 e Å^{-5}, respectively) and parallel the lengthening of their distances (Table 1). As for CD···CC interactions, bond paths and BCPs also appear in CC···CC regions, indicating bonding interactions (Figure 2b).[26] Compared to the CD···CC interactions, the bond paths in the CC···CC regions are, in general, associated with longer distances[27] (Table 1). Indeed, among the six Cl···Cl interactions, those of type-I fall in a weakness series as shown by the low values of ρ and $\nabla^2\rho$ at BCPs (Table 1). Further work is under development to obtain a deeper insight into the bonding features of these weak interactions.

In summary, halogen···halogen interactions are characterized by an anisotropic electron-density distribution around the halogen nuclei as shown by the experimental ρ maps. While both the Williams and the Nyburg models consider this anisotropy of the electron density as the origin of the halogen interaction, they differ in the interpretation of its nature (attractive vs. repulsive). The nature of the type-II interaction is evidenced when either $\Delta\rho$ or $\nabla^2\rho$ distributions are represented. These distributions clearly indicate that type-II may be understood as an interaction between nucleophilic (δ^- or CC) and electrophilic (δ^+ or CD) regions in adjacent halogen atoms. Involving, as it does, oppositely polarized regions in front of each other, the interaction is thus electrophilic–nucleophilic in nature. To this extent, the ρ, $\Delta\rho$, and $\nabla^2\rho$ distributions lead to a unique result: type-II interactions should be unambiguously considered as attractive, and this is related in a straightforward way to the Williams model.

Table 1: Cl···Cl interactions in the crystalline C_6Cl_6. ρ and $\nabla^2\rho$ are calculated at BCP.

cp	X···X	d [Å]	θ_1/θ_2 [°]	ρ [e Å^{-3}]	$\nabla^2\rho$ [e Å^{-5}]	Nature	Type
1	Cl1···Cl2	3.4343	175/117	0.06	0.6	CD···CC	II
2	Cl2···Cl3	3.4618	175/124	0.05	0.6	CD···CC	II
5	Cl2···Cl2	3.6129	126/119	0.04	0.5	CC···CC	I
6	Cl3···Cl3	3.6238	125/104	0.04	0.5	CC···CC	I
3	Cl3···Cl1	3.6542	171/123	0.03	0.4	CD···CC	II
4	Cl1···Cl1	3.8132	132/107	0.03	0.3	CC···CC	I

Experimental Section

Single crystals of C_6Cl_6 were grown at 50 °C by sublimation. X-ray diffraction data were collected on a Enraf–Nonius diffractometer with an APEX-II CCD detector: radiation $\lambda(Mo_{K\alpha})$, $T = 100(2)$ K (Oxford Cryosystems N_2 open flow cryostat), $a = 7.9724(2)$, $b = 3.7626(2)$, $c = 14.6851(2)$ Å, $\beta = 92.456(1)°$, $V = 440.1(1)$ Å^3, monoclinic space group $P2_1/n$, 90758 reflections collected up to $(\sin\theta/\lambda)_{max} = 1.2$ Å^{-1} using ω scans (scan width of 1° per frame repeated at eight different ϕ positions yielding to a completeness of data sets that exceeds 99.6%). Integration of frames and data reduction were performed with DENZO program.[28a] The absorption correction was carried out by using a Gaussian numerical integration.[28b] The integrated reflections were averaged[28c] to 5846 independents ($R_{int} = 0.041$). 2778 reflections having $I \geq 3\sigma(I)$ were used in the multipolar least-squares refinement: $R1 = 0.0104$, $R_w = 0.0130$, GOF = 0.90. The multipolar $\rho(\mathbf{r})$ model was expanded up to hexadecapolar order ($l = 4$) for the three independent chlorine atoms and up to octupolar order ($l = 3$) for the three independent C atoms. For Cl atoms, most significant multipoles correspond to $y_{lm\pm}$terms with $lm\pm = 20, 22+, 31+$, and $33+$. The final $\rho(\mathbf{r})$ model was therefore based on multipolar expansions up to octupolar level ($l = 3$) for C atoms and on these four multipolar terms for Cl atoms. The $(n_l\,;\zeta)$ parameters defining the Slater-type radial functions are (2, 2, 3 for $l = 1, 2, 3$; 3.0 bohr^{-1}) for C and (4, 6 for $l = 2, 3$; 4.4 bohr^{-1}) for Cl. CCDC 710514 contains the supplementary crystallographic data for this paper. These data can be obtained free of charge from The Cambridge Crystallographic Data Centre via www.ccdc.cam.ac.uk/data_request/cif.

Received: November 25, 2008
Revised: February 3, 2009
Published online: April 16, 2009

Keywords: charge density · chlorine · crystal engineering · halogen bonding · supramolecular chemistry

[1] a) D. E. Williams, *J. Chem. Phys.* **1967**, *47*, 4680–4684; b) A. I. Kitaigorodskii in *Advances in Structure Research by Diffraction Methods*, *Vol. 3* (Eds.: R. Brill, R. Mason), Pergamon, Oxford, **1970**, pp. 173–247.

[2] G. R. Desiraju, *Crystal Engineering: The Design of Organic Solids*, Elsevier, Amsterdam, **1989**, pp. 177–178.

[3] K. Yamasaki, *J. Phys. Soc. Jpn.* **1962**, *17*, 1262–1267.

[4] D. E. Williams, L. Y. Hsu, *Acta Crystallogr. Sect. A* **1985**, *41*, 296–301.

[5] a) S. C. Nyburg, W. Wong-Ng, *Inorg. Chem.* **1979**, *18*, 2790–2791; b) S. C. Nyburg, W. Wong-Ng, *Proc. R. Soc. London Ser. A* **1979**, *367*, 29–45.

[6] For some representative papers see: a) J. A. R. P. Sarma, G. R. Desiraju, *Acc. Chem. Res.* **1986**, *19*, 222–229; b) S. L. Price, A. J. Stone, J. Lucas, R. S. Rowland, A. E. Thornley, *J. Am. Chem. Soc.* **1994**, *116*, 4910–4918; c) O. V. Grineva, P. M. Zorky, *Cryst. Rep.* **2000**, *45*, 633–639; d) C. E. Marjo, A. N. M. M. Rahman, R. Bishop, *Tetrahedron* **2001**, *57*, 6289–6293; e) L. Brammer, G. M. Esparallargas, S. Libri, *CrystEngComm* **2008**, *10*, 1712–1727; f) B. K. Saha, A. Nangia, J.-F. Nicoud, *Cryst. Growth Des.* **2006**, *6*, 1278–1281.

[7] P. García, S. Dahaoui, C. Katan, M. Souhassou, C. Lecomte, *Faraday Discuss.* **2007**, *135*, 217–235, 125–149, 237–259.

[8] a) T. Sakurai, M. Sundaralingam, G. A. Jeffrey, *Acta Crystallogr.* **1963**, *16*, 354–363; b) G. R. Desiraju, R. Parthasarathy, *J. Am. Chem. Soc.* **1989**, *111*, 8725–8726.

[9] V. R. Pedireddi, D. S. Reddy, B. S. Goud, D. C. Craig, A. D. Rae, G. R. Desiraju, *J. Chem. Soc. Perkin Trans. 2* **1993**, 2353–2360.

[10] A. Anthony, G. R. Desiraju, R. K. R. Jetti, S. S. Kuduva, N. N. L. Madhavi, A. Nangia, R. Thaimattam, V. R. Thalladi, *Cryst. Eng.* **1998**, *1*, 1–18; B. K. Saha, R. K. R. Jetti, L. S. Reddy, S. Aitipamula, A. Nangia, *Cryst. Growth Des.* **2005**, *5*, 887–899.

[11] C. M. Reddy, M. T. Kirchner, R. C. Gundakaram, K. A. Padmanabhan, G. R. Desiraju, *Chem. Eur. J.* **2006**, *12*, 2222–2234.

[12] A first experimental electron-density analysis mainly focused on I···N interactions was performed by R. Bianchi, A. Forni, T. Pilati, *Chem. Eur. J.* **2003**, *9*, 1631–1638.

[13] a) N. K. Hansen, P. Coppens, *Acta Crystallogr. Sect. A* **1978**, *34*, 909–921; b) B. Guillot, L. Viry, R. Guillot, C. Lecomte, C. Jelsch, *J. Appl. Crystallogr.* **2001**, *34*, 214–223; c) C. Jelsch, B. Guillot, A. Lagoutte, C. Lecomte, *J. Appl. Crystallogr.* **2005**, *38*, 38–54.

[14] P. García, PhD Thesis, University of Nancy (France), **2007**.

[15] R. F. W. Bader, *Atoms in Molecules—a Quantum Theory*, Oxford Univ. Press, **1990**.

[16] Interatomic zero-flux surfaces S are defined from the points $\mathbf{r}$ holding the equation: $\nabla\rho(\mathbf{r})\cdot\mathbf{n}(\mathbf{r}) = 0\ \forall\mathbf{r} \in S$, where $\mathbf{n}$ is the unit vector perpendicular to S at $\mathbf{r}$.

[17] R. F. W. Bader, *Phys. Rev. B* **1994**, *49*, 13348–13356.

[18] While the existence of a $\rho(\mathbf{r})$ saddle conformation between nuclei and the concomitant BCP is a necessary condition, it may not be a sufficient one. For instance, isolated spherical atoms placed at the observed nuclear positions in a molecule also generate basins and BCPs. However, in this case, the topological regions cannot be considered as quantum open systems because the molecular properties cannot be predicted by quantum mechanics.

[19] E. Espinosa, M. Souhassou, H. Lachekar, C. Lecomte, *Acta Crystallogr. Sect. B* **1999**, *55*, 563–572.

[20] E. Espinosa, I. Alkorta, J. Elguero, E. Molins, *J. Chem. Phys.* **2002**, *117*, 5529–5542.

[21] The weakness of halogen···halogen interactions can be estimated by comparing them with the stronger halogen···X (X = O, N) interactions, which are themselves only about twice as strong as typical C–H···O interactions: A. Gavezzotti, *Mol. Phys.* **2008**, *106*, 1473–1485.

[22] The internal and external estimates of the experimental average $\rho(\mathbf{r})$ error are approximately 0.03 e Å^{-3}, as calculated from: D. W. J. Cruickshank, *Acta Crystallogr.* **1949**, *2*, 65–82.

[23] R. F. W. Bader, R. J. Gillespie, P. J. MacDougall, *J. Am. Chem. Soc.* **1988**, *110*, 7329–7336.

[24] V. G. Tsirelson, P. F. Zhou, T.-H. Tang, R. F. W. Bader, *Acta Crystallogr. Sect. A* **1995**, *51*, 143–153.

[25] R. F. W. Bader, *Chem. Rev.* **1991**, *91*, 893–928.

[26] While similar features are observed in the theoretical analysis of solid Cl_2, CC···CC interactions could not be evidenced from the multipolar $\rho(\mathbf{r})$ model fitted to the experimental structure factors of this compound: E. D. Stevens, *Mol. Phys.* **1979**, *37*, 27–45 (see reference [24]).

[27] The bond path created between two CC regions is typically the consequence of a secondary interaction when the CCs of the atomic VSCC are placed close to each other as resulting from the driving forces of primary CC···CD interactions (see reference [24]).

[28] a) Z. Otwinowski, W. Minor, *Methods Enzymol.* **1997**, *276*, 307–326; b) G. T. DeTitta, *J. Appl. Crystallogr.* **1985**, *18*, 75–79; c) R. H. Blessing, *Crystallogr. Rev.* **1987**, *1*, 3–58.

